PACS numbers: 52.25.Jm; 52.38.Kd
DOI: 10.1070/QE2002v032n01ABEH002119

Ionisation refraction as the cause of space – time modulation of a short intense laser pulse

M.V.Chegotov

***Abstract*. The three-dimensional dynamics of the propagation of a short intense laser pulse in an ionising material is analysed. The modulation of the temporal profile of the laser pulse caused by the essentially three-dimensional dynamics of its propagation is studied using an analytic model proposed. The criterion for realisation of various scenarios of the pulse propagation in an ionising gas is suggested. The numerical self-consistent analysis of the nonlinear propagation of the pulse in the ionising material showed the correctness of conclusions of the simplest analytic model.**

Keywords: *ionisation refraction, space – time modulation, short laser pulse*.

1. Introduction

Great interest in the study of the propagation of short intense laser pulses in ionising materials is caused by a broad scope of applications of these pulses. This is, in particular, the generation of a wake plasma wave accelerating electrons at the ionisation front [1, 2], the generation of the high laser frequency harmonics upon ionisation of the matter [3], and the development of sources of highly charged low-temperature ions [4]. The space – time evolution of a laser pulse is one of the most important factors determining the efficiency of the use of laser pulses in these applications.

The propagation of short intense laser pulses in ionising media has been studied in many papers. In particular, the authors of paper [5] studied the propagation of a laser pulse in a partially ionised medium and the influence of the motion of different electrons (bound and free electrons) on the propagation process; ionisation and a substantial change in the conditions of the pulse propagation in the substance ionised by the pulse were neglected in [5]. In paper [5], the modification of the increments of well-known parametric instabilities and the appearance of new types of instabilities in the presence of bound electrons were discussed (see also paper [6]). However, the theory presented in these papers is similar to a linear analysis of the stability of propagation of an electromagnetic radiation in an ionised medium used in paper [7], a plane wave being considered as the main state of the laser field being studied for stability.

The results of the numerical analysis of the one-dimensional propagation of a laser pulse in an ionising gas (see, for example, Fig. 1 in paper [8]) demonstrate the appearance and development of the modulation of the temporal profile of the pulse during its propagation in the gas. In paper [8] (for the one-dimensional formulation of the problem), this modulation is caused by absorption of radiation when bound electrons acquire the residual energy upon ionisation. Note that such energy losses do not describe total ionisation losses, which include losses related to the overcoming of the ionisation potential by an electron [9], which were neglected in paper [8]. Under the conditions considered in paper [8], the losses related to the residual energy and the ionisation potential are close. The combined action of these losses results in the formation of a hole in the temporal profile of the laser pulse. In this case, after a sufficiently deep penetration into gas with many-electron atoms, the laser pulse acquires the shape modulated in time [9].

The necessity of the three-dimensional formulation of the problem for analysing the propagation of the laser pulse in an ionising gas was demonstrated both theoretically and experimentally in paper [10]. It was shown that the ionisation of the gas changes the focusing, resulting in the displacement of the focus. However, the effect of ionisation on the space – time shape of the pulse was not considered.

In this paper, we study the modulation of the temporal profile of the laser pulse caused by the three-dimensional diffraction of radiation by plasma bunches (ionisation refraction [11]). Such modulation appears already at small penetration depths of the pulse into substance, when the effect of ionisation losses [9] on the pulse shape can be neglected. A low power of the laser pulse compared to the threshold power of self-focusing makes the mechanism of space – time modulation of the pulse studied in this paper different from mechanisms discussed in papers [8, 12, 13]. The pulse power in paper [8] (for non-one-dimensional formulation of the problem) exceeded the threshold power of relativistic self-focusing, while in papers [12, 13] the radius of the laser beam was so large that the pulse power exceeded the threshold power of self-focusing in a neutral gas. The propagation of short intense laser pulses in ionising gases was also studied numerically in paper [14], where the formation of circular structures was demonstrated in the laser radiation transmitted through the gas.

M.V.Chegotov Institute for High Energy Densities, Joint Institute of High Temperatures, Russian Academy of Sciences,
Izhorskaya ul. 13/19, 127412 Moscow, Russia;
e-mail: chegotov@hedric.msk.su

Received 13 September 2001
Kvantovaya Elektronika **32** (1) 19 – 26 (2002)
Translated by M.N.Sapozhnikov

2. Basic equations

Assuming that the electromagnetic field of a laser pulse propagating along the z axis is transverse, the equation for the electric field $\vec{\mathscr{E}}(z, \boldsymbol{r}_\perp, t)$ of laser radiation has the form

$$\frac{1}{c^2}\frac{\partial^2\vec{\mathscr{E}}}{\partial t^2} - \frac{\partial^2\vec{\mathscr{E}}}{\partial z^2} - \Delta_\perp\vec{\mathscr{E}} + \frac{4\pi}{c^2}\frac{\partial \boldsymbol{J}}{\partial t} = 0.$$

Here, c is the speed of light; $\Delta_\perp = \partial^2/\partial x^2 + \partial^2/\partial y^2$; $\boldsymbol{r}_\perp = \boldsymbol{e}_x x + \boldsymbol{e}_y y$; $\boldsymbol{e}_x$ and $\boldsymbol{e}_y$ are the unit vectors along axes x and y, respectively; and $\boldsymbol{J}$ is the electron current density. Below, we will neglect nonlinearities during the motion of electrons in the laser-wave field. Such an approximation is applicable for comparatively small $\mathscr{E}$, when the inequality $e^2\mathscr{E}^2/m^2\omega_0^2 \ll c^2$ is fulfilled, where e and m are the electron charge and mass, respectively, and ω_0 is the laser radiation frequency. In addition, by studying the effect of ionisation on the propagation of laser radiation, we will neglect the ionisation current [2]. This is possible because the amplitudes of harmonics excited by this current are comparatively small, and the ionisation losses have a substantial effect on the ionising laser pulse only after comparatively long propagation of the laser pulse in matter [9].

Then, the equation for the density of free electrons appearing due to tunnel ionisation will take the form

$$\frac{\partial \boldsymbol{J}}{\partial t} = \frac{e^2 n_\mathrm{e}}{m}\vec{\mathscr{E}},$$

where $n_\mathrm{e}(z, \boldsymbol{r}_\perp, t)$ is the free-electron density. Note that the right-hand side of this equation is a nonlinear function of the laser-field strength because the free-electron density increasing with time due to ionisation is a strongly nonlinear function of $\mathscr{E}$.

To describe the space–time evolution of the electric field of laser radiation polarised along $\boldsymbol{e}_x$, we represent $\vec{\mathscr{E}}(z, \boldsymbol{r}_\perp, t)$ in the form

$$\vec{\mathscr{E}}(z, \boldsymbol{r}_\perp, \xi) = \frac{1}{2}\boldsymbol{e}_x E(z, \boldsymbol{r}_\perp, \xi)\exp(-\mathrm{i}\omega_0\xi) + \mathrm{c.c.}$$

and will use the parabolic equation for the field amplitude $E(z, \boldsymbol{r}_\perp, \xi)$ slowly varying over the laser period $2\pi/\omega_0$ and the wavelength $\lambda_0 = 2\pi c/\omega_0$:

$$\frac{\partial E}{\partial z} - \mathrm{i}\frac{c}{2\omega_0}\Delta_\perp E + \mathrm{i}\frac{\omega_\mathrm{p}^2}{2\omega_0 c}E = 0, \tag{1}$$

where $\omega_\mathrm{p}^2 = 4\pi e^2 n_\mathrm{e}(z, \boldsymbol{r}_\perp, t)/m$; and $\xi = t - z/c$ is the time in the coordinate system coupled to the momentum. We neglected in equation (1), in particular, the dispersion of the electromagnetic wave assuming that the electron density is low: $n_\mathrm{e} \ll n_\mathrm{c} = m\omega_0^2/4\pi e^2$.

We will describe the dynamics of the electron density using the system of equations

$$\frac{\partial n_\mathrm{e}}{\partial \xi} = \Gamma = \sum_a \sum_{k=0}^{Z_a - 1} W_{ak}(E) n_{ak},$$

$$\frac{\partial n_{a0}}{\partial \xi} = -W_{a0} n_{a0}, \quad \frac{\partial n_{ak}}{\partial \xi} = -W_{ak} n_{ak} + W_{ak-1} n_{ak-1}, \tag{2}$$

$$\frac{\partial n_{aZ_a}}{\partial \xi} = W_{aZ_a-1} n_{aZ_a-1}, \quad k = 1, \ldots, Z_a - 1,$$

where Z_a is the nuclear charge of an atom of matter a; n_{ak} is the ion density of matter a with the ionisation degree k ($k = 0$ corresponds to a neutral atom); $W_{ak}(E)$ is the probability of ionisation of an ion with the ionisation degree k to an ion with the ionisation degree $k + 1$, which is determined by the Ammosov–Krainov formula [15]

$$W_{ak}(E) = \omega_\mathrm{at}\sqrt{3}\left(\frac{\mathrm{e}}{\pi}\right)^{3/2}\frac{(k+1)^2}{n_*^{4.5}}\left[4\mathrm{e}\frac{(k+1)^3}{n_*^4}\frac{E_\mathrm{at}}{|E|}\right]^{2n_* - 1.5}$$

$$\times \exp\left[-\frac{2}{3}\frac{(k+1)^3}{n_*^3}\frac{E_\mathrm{at}}{|E|}\right]; \tag{3}$$

$n_* = (k+1)(U_\mathrm{H}/U_{ak})^{1/2}$; U_H is the potential of ionisation of a hydrogen atom from the ground state; $E_\mathrm{at} \approx 5.1 \times 10^9$ V cm^{-1} is the atomic field strength; U_{ak} is the potential of ionisation of an ion of matter a with the ionisation degree k to an ion with the ionisation degree $k + 1$; $\omega_\mathrm{at} \approx 4.1 \times 10^{16}$ s^{-1} is the atomic frequency; $\mathrm{e} \approx 2.72$ is the base of natural logarithms.

We will write the boundary condition for equation (1) in the form

$$E(z = 0, \boldsymbol{r}_\perp, \xi) = E_0 \exp\left(-\frac{r_\perp^2}{r_0^2} - \frac{\xi^2}{\tau^2}\right), \tag{4}$$

which corresponds to the focusing with the radius r_0 of a Gaussian pulse with the characteristic duration τ at the boundary $z = 0$. As the initial condition for equations (2), we take the condition

$$n_{a0}(z, \boldsymbol{r}_\perp, \xi = -\infty) = n_a^{(0)} = \mathrm{const},$$

$$n_{ak}(z, \boldsymbol{r}_\perp, \xi = -\infty) = 0, \quad k = 1, 2, \ldots, Z_a - 1, \tag{5}$$

which corresponds to the ionised gas in the absence of the laser pulse.

3. The simplest model

Upon tunnel ionisation, the free-electron density n_e quite strongly depends on space–time variables. The ionisation of ions of matter a with the ionisation degree k to ions with the ionisation degree $k + 1$ lasts in time for several laser periods and occurs in space in the region of several laser wavelengths (Fig. 1). Because the ionisation is strongly localised in the vicinity of some intensity of laser radiation, it is characterised by the threshold intensity I_{ak}^th, which can be quite accurately estimated from the relation $I_{ak}^\mathrm{th} = cU_{ak}^4/[128\pi\mathrm{e}^6(k+1)^2]$ [9]. This allows us to consider as the simplest model of ionisation at the leading edge of the pulse ($\xi \leqslant 0$) the following model

$$n_\mathrm{e} = \sum_a n_a^{(0)} \sum_{k=0}^{Z_a - 1} \theta\left(I - I_{ak}^\mathrm{th}\right), \tag{6}$$

where $\theta(p) = 0$ for $p < 0$ and 1 for $p \geqslant 0$. For small depths of penetration of a laser pulse in matter $z < z_\mathrm{R}$ ($z_\mathrm{R} = \omega_0 r_0^2/2c$ is the Rayleigh length), the spatial shape of the pulse (4) is weakly transformed. In this case, the distribution of the electron density (6) in coordinates $\boldsymbol{r}_\perp, \xi$ for the leading edge of the pulse ($\xi \leqslant 0$) has the form of embedded ellipsoids

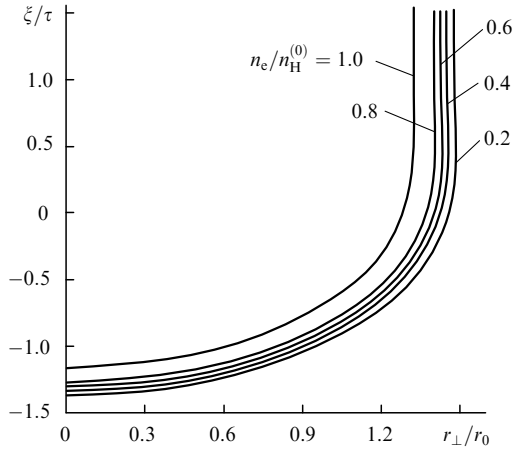

Figure 1. Level lines of the electron density $n_e/n_H^{(0)}$ in hydrogen with the density $n_H^{(0)} = 10^{18}$ cm^{-3} in the pulse frame of reference ξ, $r_\perp$ for $z = 0$ and the following parameters of a Gaussian pulse: $I_0 = 10^{16}$ W cm^{-2}, the HWHM duration of the electric field modulus $T = 40$ fs [$\tau = T/(2\ln 2)^{1/2} \approx 34$ fs], the wavelength $\lambda_0 = 0.8$ μm, and the radius $r_0 = 53$ μm.

$$\frac{r_\perp^2}{r_0^2} + \frac{\xi^2}{\tau^2} = \frac{1}{2}\ln\left(\frac{I_0}{I_{ak}^{\text{th}}}\right), \tag{7}$$

where $I_0 = c|E_0|^2/8\pi$. Because we neglect recombination processes due to the low gas density, the distribution of the electron density n_e for $\xi > 0$ has the form of embedded cylinders with radii

$$R_{ak}(\xi > 0) = R_{ak}(0) = r_0\left[\frac{1}{2}\ln\left(\frac{I_0}{I_{ak}^{\text{th}}}\right)\right]^{1/2}, \tag{8}$$

the electron density increasing on passing from a cylinder with a greater radius to a cylinder with a smaller radius (see Fig. 2). Because the boundaries of the electron density in the radial direction are comparatively distinct, we can say that a plasma waveguide is formed due to ionisation of the gas by laser pulses. From the point of view of expression (8), the equality (7) can be interpreted as follows: an arbitrary cross section of the pulse $\xi = \text{const} \leqslant 0$ propagates in a medium in which the electron density produced in ionisation is distributed along a cylinder with the axis z and

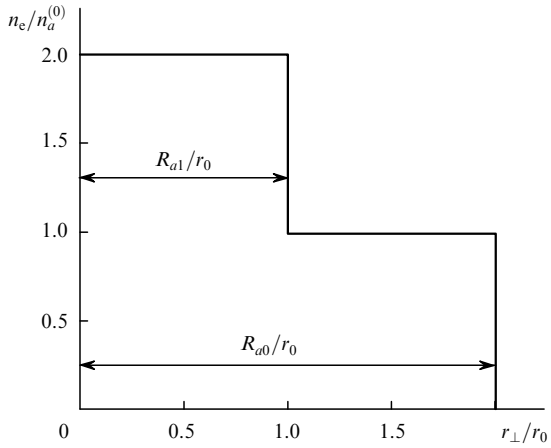

Figure 2. Distribution of the electron density perpendicular to the z axis in the model (6).

the characteristic dependence on the transverse radius $r_\perp$ shown in Fig. 2, where radii R_{ak} depend on the given position ξ on the temporal profile:

$$R_{ak}(\xi) = r_0\left[\frac{1}{2}\ln\left(\frac{I_0}{I_{ak}^{\text{th}}}\right) - \frac{\xi^2}{\tau^2}\right]^{1/2}. \tag{9}$$

Therefore, each cross section $\xi = \text{const}$ of the temporal profile of the pulse in an ionising matter propagates in a plasma waveguide with the transverse distribution of the electron density, which is close to a step distribution (see Fig. 2), whose radii depend on the position ξ and are determined in our case by expression (9).

We will solve within the framework of this model the equation (1) with the boundary condition (4). The profile of the electron density perpendicular to the laser pulse propagation appearing in equation (1) has a characteristic form shown in Fig. 2, where the radii R_{ak} at the leading edge of the laser pulse ($\xi \leqslant 0$) depend on ξ and are determined by expression (9). Because the propagation lengths are small within the framework of our model: $z/z_R \equiv s < 1$, we find the solution of (1) in the first order of the expansion in the parameter $n_e/n_c \ll 1$:

$$E(s, \boldsymbol{r}_\perp, \xi) = E^{(0)}(s, \boldsymbol{r}_\perp, \xi) - \frac{\omega_0^2}{4\pi c^2}\int_0^s \frac{\mathrm{d}s'}{s - s'}\int \mathrm{d}^2\boldsymbol{r}_\perp' \frac{n_e(\boldsymbol{r}_\perp', \xi)}{n_c}$$

$$\times E^{(0)}(s, \boldsymbol{r}_\perp', \xi)\exp\left[\mathrm{i}\frac{1}{r_0^2}\frac{(\boldsymbol{r}_\perp - \boldsymbol{r}_\perp')^2}{s - s'}\right], \tag{10}$$

where

$$E^{(0)}(s, \boldsymbol{r}_\perp, \xi) = \frac{E_0}{1 + \mathrm{i}s}\exp\left(-\frac{\boldsymbol{r}_\perp^2/r_0^2}{1 + \mathrm{i}s} - \frac{\xi^2}{\tau^2}\right)$$

is the freely diffracting solution of equation (1) with the boundary condition (4).

Let us study the behaviour of the intensity of field (10) at the axis $\boldsymbol{r}_\perp = 0$ of the beam. To do this, we calculate the integral over the transverse cross section in (10) taking into account (6):

$$E(s, \boldsymbol{r}_\perp = 0, \xi) = E^{(0)}(s, \boldsymbol{r}_\perp = 0, \xi)$$

$$\times\left\{1 + \mathrm{i}\left(\frac{\omega_0 r_0}{2c}\right)^2 \sum_a \frac{n_a^{(0)}}{n_c}\sum_{k=0}^{Z_a - 1}\theta(\xi - \xi_{ak}^{\text{th}})\right.$$

$$\left.\times\int_0^s\left\{\exp\left[\mathrm{i}\frac{R_{ak}^2(\xi)}{r_0^2}\frac{1 + \mathrm{i}s}{(s - s')(1 + \mathrm{i}s')}\right] - 1\right\}\mathrm{d}s'\right\}, \quad \xi \leqslant 0,$$

$$E(s, \boldsymbol{r}_\perp = 0, \xi) = E^{(0)}(s, \boldsymbol{r}_\perp = 0, \xi)$$

$$\times\left\{1 + \mathrm{i}\left(\frac{\omega_0 r_0}{2c}\right)^2 \sum_a \frac{n_a^{(0)}}{n_c}\sum_{k=0}^{Z_a - 1}\theta(I_0 - I_{ak}^{\text{th}})\times\right.$$

$$\left.\times\int_0^s\left\{\exp\left[\mathrm{i}\frac{R_{ak}^2(0)}{r_0^2}\frac{1 + \mathrm{i}s}{(s - s')(1 + \mathrm{i}s')}\right] - 1\right\}\mathrm{d}s'\right\}, \quad \xi > 0,$$

where ξ_{ak}^{th} corresponds to the position of the threshold intensity on the leading edge ($\xi \leqslant 0$) of the temporal profile of the pulse for $r_\perp = 0$. By taking the square of modulus

from this expression, we obtain in the approximation linear in n_e/n_c

$$|E(s,\boldsymbol{r}_\perp=0,\xi)|^2=|E^{(0)}(s,\boldsymbol{r}_\perp=0,\xi)|^2$$

$$\times\left\{1-\frac{1}{2}\left(\frac{\omega_0 r_0}{c}\right)^2\sum_a\frac{n_a^{(0)}}{n_c}\sum_{k=0}^{Z_a-1}\theta(\xi-\xi_{ak}^{th})\int_0^s\exp\left(-\frac{R_{ak}^2(\xi)/r_0^2}{1+s'^2}\right)\right.$$

$$\left.\times\sin\left[\frac{R_{ak}^2(\xi)}{r_0^2}\frac{1+ss'}{(s-s')(1+s'^2)}\right]ds'\right\},\quad \xi\leqslant 0,$$

$$|E(s,\boldsymbol{r}_\perp=0,\xi)|^2=|E^{(0)}(s,\boldsymbol{r}_\perp=0,\xi)|^2 \tag{11}$$

$$\times\left\{1-\frac{1}{2}\left(\frac{\omega_0 r_0}{c}\right)^2\sum_a\frac{n_a^{(0)}}{n_c}\sum_{k=0}^{Z_a-1}\theta(I_0-I_{ak}^{th})\int_0^s\exp\left(-\frac{R_{ak}^2(0)/r_0^2}{1+s'^2}\right)\right.$$

$$\left.\times\sin\left[\frac{R_{ak}^2(0)}{r_0^2}\frac{1+ss'}{(s-s')(1+s'^2)}\right]ds'\right\},\quad \xi>0,$$

For small penetration depths ($s^2R_{ak}^2(\xi)/r_0^2<1$), expression (11) can be simplfied:

$$|E(s,\boldsymbol{r}_\perp=0,\xi)|^2=|E^{(0)}(s,\boldsymbol{r}_\perp=0,\xi)|^2$$

$$\times\left\{1-\frac{s}{2}\left(\frac{\omega_0 r_0}{c}\right)^2\sum_a\frac{n_a^{(0)}}{n_c}\sum_{k=0}^{Z_a-1}\theta(\xi-\xi_{ak}^{th})\exp[-su_{ak}(s,\xi)]\right.$$

$$\left.\times F(u_{ak}(s,\xi))\right\},\quad \xi\leqslant 0,$$

$$|E(s,\boldsymbol{r}_\perp=0,\xi)|^2=|E^{(0)}(s,\boldsymbol{r}_\perp=0,\xi)|^2 \tag{12}$$

$$\times\left\{1-\frac{s}{2}\left(\frac{\omega_0 r_0}{c}\right)^2\sum_a\frac{n_a^{(0)}}{n_c}\sum_{k=0}^{Z_a-1}\theta(I_0-I_{ak}^{th})\exp[-su_{ak}(s,0)]\right.$$

$$\left.\times F(u_{ak}(s,0))\right\},\quad \xi>0$$

Here, $u_{ak}(s,\xi)=R_{ak}^2(\xi)/(r_0^2 s)$; $F(x)=\sin(x)-x\mathrm{Ci}(x)$;

$$\mathrm{Ci}(x)=-\int_x^\infty\frac{\cos t}{t}dt$$

is the integral cosine [16]. If the laser pulse propagated in a preliminary prepared plasma waveguide with a fixed radius ($R=\mathrm{const}$), then the temporal profile of the pulse would be only determined by the temporal profile of a freely diffracting pulse and thereby by the time dependence of the field at the boundary [see (4)].

However, the radius R in an ionising material is a function of the position ξ on the leading edge of the pulse [see (9)]. For this reason, the leading edge of the pulse becomes modulated upon the pulse propagation into an ionised material. Note that, within the framework of our model, the trailing edge of the pulse propagates in a preliminary formed plasma waveguide ($\xi>0$). This results in the absence of modulation of the trailing edge of the pulse [see (11), (12) for $\xi>0$].

Fig. 3 shows the dependence (12) on ξ for the leading edge of the pulse with the maximum intensity $I_0=10^{16}$ W cm^{-2}, the HWHM duration of the electric field modulus

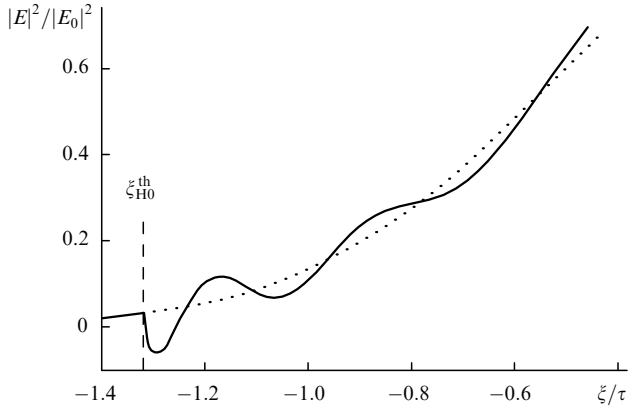

Figure 3. Dependence (12) (solid curve) and the dependence of the initial profile of the pulse (dashed curve) on ξ. The parameters of the pulse and gas are as in Fig. 1; the time ξ is measured from the maximum of the initial profile of the pulse; the penetration depth of the pulse inside the gas is $z=0.1z_R$.

$T=40$ fs, the wavelength $\lambda_0=0.8$ μm, and the radius $r_0=53$ μm penetrated to the depth $z=0.1z_R$ in hydrogen ($U_{H0}=13.6$ eV, $I_{H0}^{th}=3.1\times10^{14}$ W cm^{-2}) with the initial density of atoms $n_H^{(0)}=10^{18}$ cm^{-3}. The chosen threshold intensity I_{H0}^{th} takes into account the ionisation dynamics in the pulse field and differs from the intensity 1.4×10^{14} W cm^{-2} predicted by the above-mentioned formula of the stationary theory (cf. [9]).

Note a number of features of the dependence of the intensity at the beam axis on ξ. They are mainly determined by the behaviour of the function $F(x)$ presented in Fig. 4. Near the threshold intensity of ionisation [in the vicinity ξ_{ak}^{th} ($\xi>\xi_{ak}^{th}$) in Fig. 3], the ionisation intensity rapidly falls. Away from the threshold intensity, with increasing ξ, the pulse field oscillates with respect to its initial shape, the oscillation period in ξ increasing, while their amplitude decreases.

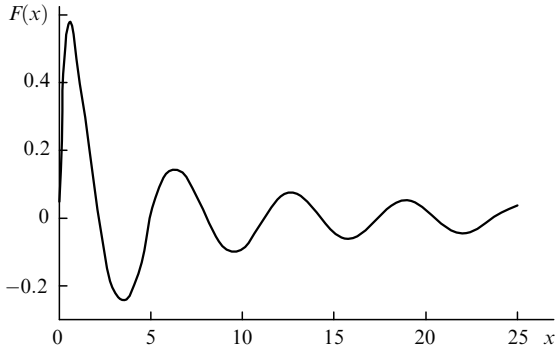

Figure 4. Function $F(x)=\sin x-x\mathrm{Ci}(x)$.

A rapid decrease in the field intensity in the vicinity of ξ_{ak}^{th} means that the laser pulse diffracts efficiently from a plasma waveguide with a small radius. Because in this case the field intensity $I=c|E|^2/8\pi$ becomes lower than the threshold intensity I_{ak}^{th} [$I_{ak}^{th}\equiv I(\xi_{ak}^{th})=I(\xi_{ak}^{NL})$] in the region $\xi_{ak}^{th}<\xi<\xi_{ak}^{NL}$, the simplest model presented here proves to be too crude for the description of the nonlinear self-consistent balance of ionisation and diffraction in plasma bunches of small radius in the region (ξ_{ak}^{th}, ξ_{ak}^{NL}). The point

$\xi_{ak}^{\rm NL}$ is found from the condition $I = I_{ak}^{\rm th}$. Nevertheless, we will see below from the numerical self-consistent analysis of the nonlinear propagation of a laser pulse in an ionising gas that the model correctly describes the tendency to rapid diffraction at the leading edge of the ionisation front in the vicinity of $\xi_{ak}^{\rm th}$. In the case of a weak penetration into a material ($s < 1$), the quantity $\xi_{ak}^{\rm NL}$ can be approximately found from the equation

$$F(u_{ak}(s,\xi)) = 0, \tag{13}$$

as the first nonzero root $u_{ak}(s,\xi_{ak}^{\rm NL}) = u^{\rm NL} \approx 2.156$ (see Fig. 4). This gives

$$\frac{\xi_{ak}^{\rm NL}}{\tau} = -\left[\frac{1}{2}\ln\left(\frac{I_0}{I_{ak}^{\rm th}}\right) - su^{\rm NL}\right]^{1/2} = -\left[\left(\frac{\xi_{ak}^{\rm th}}{\tau}\right)^2 - su^{\rm NL}\right]^{1/2}, \tag{14}$$

so that the region of efficient diffraction at the leading edge in the vicinity of the ionisation threshold increases during the pulse penetration into the matter (i.e., with increasing s).

For $\xi > \xi_{ak}^{\rm NL}$, the laser-field intensity is sufficient for ionisation. The positions of the maxima of the deviation of $|E|^2$ from $|E^{(0)}|^2$ on the axis ξ are close to the extrema of the function $F(u_{ak}(s,\xi))$. The latter coincide with the zeroes of the function $\mathrm{Ci}(u_{ak})$. Because $u^{(1)} \approx 0.617$ – the first nonzero root of the equation $\mathrm{Ci}(u) = 0$ – corresponds to $\xi < \xi_{ak}^{\rm NL}$, it should be excluded. The second root $u^{(2)} \approx 3.384$ corresponds to $\xi > \xi_{ak}^{\rm NL}$; the next roots are determined by the relation $u^{(n)} \approx (n-1)\pi$ with an error better than 2 %, where $n = 3, 4, \ldots$, the error decreasing with n. Then, the coordinates $\xi_{ak}^{(n)}$ of maximum deviations from the initial pulse shape on its temporal profile are determined approximately by the expression

$$\frac{\xi_{ak}^{(n)}}{\tau} = -\left[\frac{1}{2}\ln\left(\frac{I_0}{I_{ak}^{\rm th}}\right) - su^{(n)}\right]^{1/2} = -\left[\left(\frac{\xi_{ak}^{\rm th}}{\tau}\right)^2 - su^{(n)}\right]^{1/2}. \tag{15}$$

The distances between the coordinates $\xi_{ak}^{(n)}$ and $\xi_{ak}^{(n+1)}$ of the adjacent maximum deviations increase upon approaching to the peak pulse intensity (with increasing number n). The relative amplitude of deviations at these points is

$$\varepsilon_{ak}^{(n)}(s) = \frac{|E(s,\boldsymbol{r}_\perp = 0,\xi_{ak}^{(n)})|^2 - |E^{(0)}(s,\boldsymbol{r}_\perp = 0,\xi_{ak}^{(n)})|^2}{|E^{(0)}(s,\boldsymbol{r}_\perp = 0,\xi_{ak}^{(n)})|^2}$$

$$\approx -\frac{s}{2}\left(\frac{\omega_0 r_0}{c}\right)^2 \frac{n_a^{(0)}}{n_{\rm c}} \exp(-su^{(n)}) F(u^{(n)}). \tag{16}$$

In particular, we have $F(u^{(2)}) \approx -0.24$ and $F(u^{(3)}) \approx 0.143$.

It follows from expression (15) that the spatial scale of modulation increases upon the penetration of the laser pulse into a material (with increasing s), while the maxima and minima of the relative deviation $\varepsilon_{ak}^{(n)}(s)$ shift to the pulse centre $\xi = 0$. The modulation amplitude changes nonuniformly with increasing s according to (16). For the numbers n at which $u^{(n)} > 1/s$, the quantities $\varepsilon_{ak}^{(n)}(s)$ decrease with increasing s. Therefore, the region of ionisation modulation on the temporal profile of the laser pulse decreases upon the penetration of the laser pulse into the matter and concentrates near the threshold intensity of ionisation. In this case, the modulation scale increases. This tendency in the development of ionisation modulation means the formation of a step profile of the pulse, with steps in the vicinity of points $\xi_{ak}^{\rm NL}$ [see expression (14)].

We estimate the characteristic length of the step profile as the penetration depth $z_{\rm st} = z_{\rm R}/u^{(2)} \approx 0.3 z_{\rm R}$ at which the maximum of $\varepsilon_{ak}^{(2)}(s)$ nearest to $\xi_{ak}^{\rm NL}$ is located [see (16)]:

$$\varepsilon_{ak}^{(2)}\left(\frac{1}{u^{(2)}}\right) \approx 0.013\left(\frac{\omega_0 r_0}{c}\right)^2 \frac{n_a^{(0)}}{n_{\rm c}} \equiv \delta. \tag{17}$$

The rest of the extrema (with $n \geqslant 3$) prove to be suppressed at this penetration depth because of the exponential dependence on s in (16). The lowest level of the step is equal approximately to $I_{ak}^{\rm th}$ at the point $\xi_{ak}^{\rm NL}$, while the highest level $I_{ak}^{\rm st}$ is achieved at the point $\xi_{ak}^{(2)}$. According to (17), the relative height of the step can be estimated from the expression

$$\frac{I_{ak}^{\rm st} - I_{ak}^{\rm th}}{I_{ak}^{\rm th}} \approx 0.013\left(\frac{\omega_0 r_0}{c}\right)^2 \frac{n_a^{(0)}}{n_{\rm c}}. \tag{18}$$

Note that the step height can be rather large because $\omega_0 r_0/c = 2\pi r_0/\lambda_0 \gg 1$. Remaining within the framework of the simplest model used here, we should require that the value of $\varepsilon_{ak}^{(2)}(1/u^{(2)}) = \delta$ would be smaller than or at least of the order of unity.

Therefore, if $\delta \leqslant 1$, upon the propagation of the pulse by the distance $z < z_{\rm st} \approx 0.3 z_{\rm R}$, the ionisation modulation should be manifested as the modulation of the temporal profile of the pulse with the relative amplitude that is smaller than or equal to δ. Upon approaching to $z = z_{\rm st}$, a step temporal profile of the pulse with a steep leading edge is formed. The positions $\xi_{ak}^{\rm st}$ of the leading edge ($k = 0$) and steps on the temporal profile of the pulse at $s = 1/u^{(2)}$ are determined by the relation (14)

$$\frac{\xi_{ak}^{\rm st}}{\tau} = -\left[\frac{1}{2}\ln\left(\frac{I_0}{I_{ak}^{\rm th}}\right) - \frac{u^{\rm NL}}{u^{(2)}}\right]^{1/2} \approx -\left[\frac{1}{2}\ln\left(\frac{I_0}{I_{ak}^{\rm th}}\right) - 0.637\right]^{1/2}. \tag{19}$$

Then, up to the distances $z \sim z_{\rm R}$ (when the condition $z < z_{\rm R}$ of a comparatively weak diffraction accepted in the model is violated), we can expect that the space–time profile of the pulse will change weakly. The latter is caused by the fact that the ionisation refraction of the pulse at the distance $z = z_{\rm st}$ near the ionisation threshold $\xi < \xi_{ak}^{\rm NL}$ results in the formation of both steps and more flat ionisation fronts of the electron density.

For $\delta \gg 1$, the modulation of the temporal profile of the pulse proves to be significant already at $z < z_{\rm st}$, before the formation of the step profile. Under these conditions, the ionisation modulation initiates a substantial nonlinear change in the space–time profile of the pulse.

4. Numerical analysis

We solved the system of equations (1)–(3) numerically by the methods of networks, equation (1) being solved by using the conservative symmetric scheme. The accuracy of calculations was controlled by the integral of conservation of the laser power flux at each cross section ξ. Fig. 5 shows the dependences of $|E(s,\boldsymbol{r}_\perp = 0,\xi)|^2/|E_0|^2$ and $n_{\rm e}(s,\boldsymbol{r}_\perp = 0,\xi)/n_{\rm H}^{(0)}$ on ξ for the leading edge of the pulse with the peak intensity $I_0 = 10^{16}$ W cm^{-2}, the FWHM duration of the electric field modulus $T = 40$ fs, the wavelength $\lambda_0 = 0.8$ μm and the radius $r_0 = 0.53$ μm penetrated to the depth $z = 0.1 z_{\rm R}$ in hydrogen with the initial density of atoms $n_{\rm H}^{(0)} = 10^{18}$ cm^{-3}. One can see the oscillating deviations of

$|E|^2$ from the initial temporal profile. A comparison of Figs 3 and 5 shows that the simplest model used in the previous section correctly qualitatively predicts a change in the pulse shape on the axis $\boldsymbol{r}_\perp = 0$. In this case, the spatial scales of the modulation are close to each other. However, the model modulation amplitudes are approximately two times greater than the amplitudes obtained by solving a nonlinear self-consistent problem of the pulse propagation taking diffraction into account.

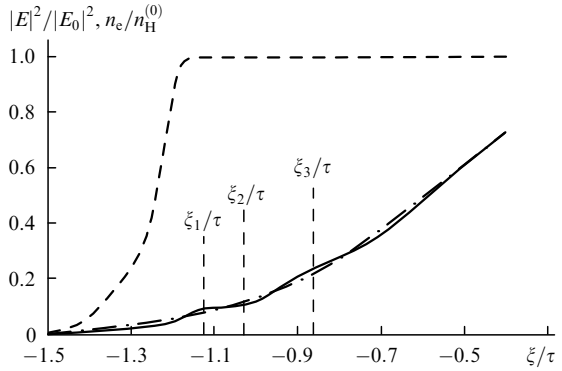

Figure 5. Dependences of $|E(s, \boldsymbol{r}_\perp = 0, \xi)|^2/|E_0|^2$ (solid curve), the initial profile of the pulse (dot-and-dash curve), and $n_e(s, \boldsymbol{r}_\perp = 0, \xi)/n_H^{(0)}$ (dashed curve) on ξ. The parameters of the pulse and gas are as in Fig. 1; the time ξ is measured from the maximum of the initial profile of the pulse; the penetration depth of the pulse inside the gas is $z = 0.1z_R$.

To understand the reason for such a difference, we consider the behaviour of the laser field and the electron density in the cross sections $\xi = \text{const}$ perpendicular to the laser beam propagation. Fig. 6 shows the dependences $n_e(r_\perp)$ and $|E(r_\perp)|^2/|E_0|^2$ for $z = 0.1z_R$ and different ξ: $\xi_1/\tau = -1.124$, $\xi_2/\tau = -1.03$, $\xi_3/\tau = -0.87$, ξ_1 and ξ_3 corresponding to the regions where $|E|^2$ increases upon modulation, while ξ_2 corresponds to the region where $|E|^2$ decrease upon modulation (Fig. 5). One can see from Fig. 6b that the modulation decrease in $|E|^2$ is caused by the refraction of laser radiation from the beam axis $\boldsymbol{r}_\perp = 0$. Because refraction occurs in a plasma channel whose walls prevent the free propagation of radiation from the axis $\boldsymbol{r}_\perp = 0$, a distinct maximum is formed away from $\boldsymbol{r}_\perp = 0$. In turn, the presence of the plasma channel results in the focusing of radiation in the vicinity of ξ_1 and ξ_3 on the temporal profile of the pulse (Figs 6a, c).

The size of the region of variable electron density over the radius $r_\perp$ in Fig. 6 is comparable with the radius of the constant-density region near $\boldsymbol{r}_\perp = 0$. This explains a more smoothed intensity modulation over ξ on the beam axis compared to that predicted by a model with sharp boundaries of n_e over the radius (see Fig. 2).

The rapid diffraction from a plasma bunch with a small transverse size at the leading edge of the pulse near the threshold intensity results in the appearance of a plateau with a comparatively low intensity. The latter decelerates ionisation and prevents the achievement of complete ionisation of gas at the leading edge of the laser pulse. The regions of the temporal profile of the pulse with a high intensity produce plasma channels with large transverse radii, resulting in the deceleration of diffraction from the electron density in these regions. As a result (see Fig. 5), the ionisation front of the electron density consists of two regions: the region of slowly increasing $n_e(\xi)$, which is controlled by strong diffraction, and the region of rapid ionisation, where the radius of the beam with the intensity above the threshold is quite large.

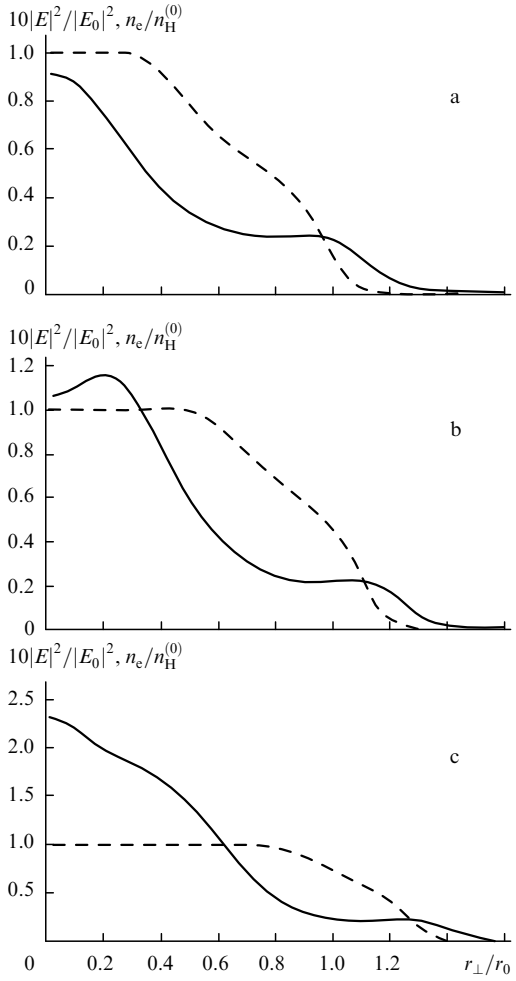

Figure 6. Dependences $10|E(r_\perp)|^2/|E_0|^2$ (solid curve) and $n_e(r_\perp)/n_H^{(0)}$ (dashed curve) for $z = 0.1z_R$ and $\xi_1/\tau = -1.124$ (a), $\xi_2/\tau = -1.03$ (b) and $\xi_3/\tau = -0.87$ (c). The parameters of the pulse and gas are as in Fig. 1.

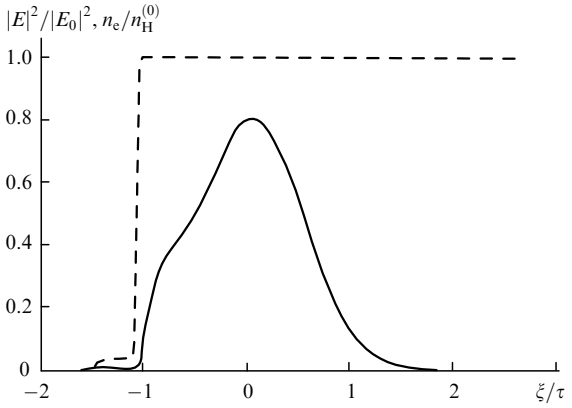

Figure 7. Dependences of $|E(s, \boldsymbol{r}_\perp = 0, \xi)|^2/|E_0|^2$ (solid curve) and $n_e(s, \boldsymbol{r}_\perp = 0, \xi)/n_H^{(0)}$ (dashed curve) on ξ. The parameters of the pulse and gas are as in Fig. 1; the time ξ is measured from the maximum of the initial profile of the pulse; the penetration depth of the pulse inside the gas is $z = 0.3z_R$.

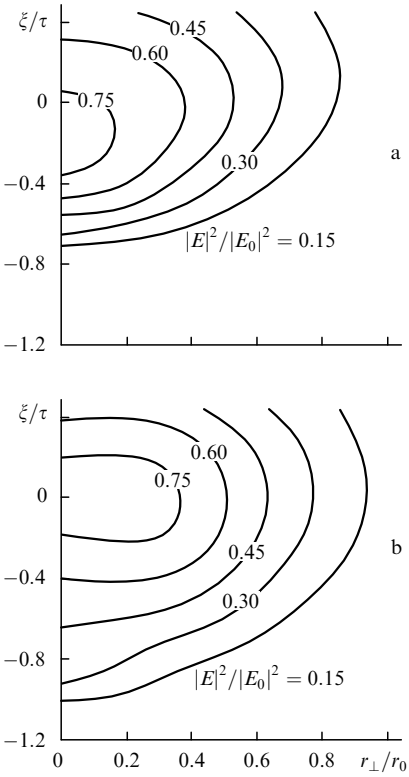

Figure 8. Level lines of $|E(s, r_\perp, \xi)|^2/|E_0|^2$ in the pulse frame of reference ξ, $r_\perp$ for $z = z_R$ (a) and $0.3z_R$ (b). The parameters of the pulse and gas are as in Fig. 1.

Note that the parameters used in Figs 5 and 6 correspond to $\delta = 1.3$ [see (17)], so that the formation of a step profile can be expected under these conditions. Indeed, one can see from Fig. 7 that the profile with a steep leading edge is formed upon propagation of the pulse inside the matter. For $I_{H0}^{th} = 3.1 \times 10^{14}$ W cm^{-2} and $I_0 = 10^{16}$ W cm^{-2}, expression (19) predicts the coordinate of this front $\xi_{H0}^{st}/\tau = -1.05$, in accordance with the front position for $z = 0.3z_R$ in Fig. 7. Fig. 8a shows the space–time distribution of the pulse intensity normalised to I_0 for a deeper penetration of the pulse into the matter, i.e., for $z = z_R$. For comparison, Fig. 8b shows the distribution of the pulse intensity for $z = 0.3z_R$. One can easily see that the space–time profiles of the pulse at these distances are very close to each other.

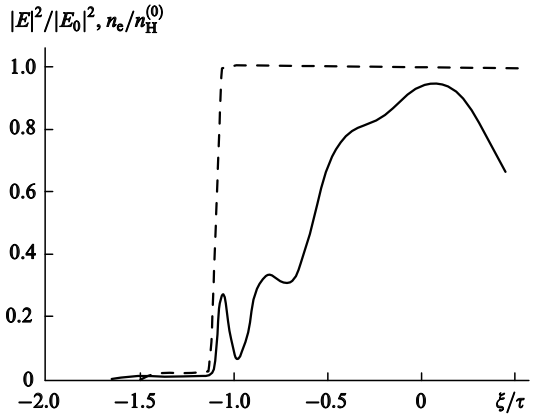

Figure 9. Dependences of $|E(s, r_\perp = 0, \xi)|^2/|E_0|^2$ (solid curve) and $n_e(s, r_\perp = 0, \xi)/n_H^{(0)}$ (dashed curve) on ξ in hydrogen for $n_H^{(0)} = 9 \times 10^{18}$ cm^{-3}. The parameters of the pulse and gas are as in Fig. 1; the time ξ is measured from the maximum of the initial profile of the pulse; the penetration depth of the pulse inside the gas is $z = 0.1z_R$.

According to expression (12), the amplitude of ionisation modulation is determined by the dimensionless parameter $A = (\omega_0 r_0/c)^2 n_a^{(0)}/n_c$ [see also (18)]. For the examples considered above, $A = 100$. This quantity also determines the ratio of the laser pulse power P to the threshold power P_c of relativistic self-focusing. For the above examples, this ratio is comparatively small: $P/P_c \approx 0.015$. Such a small ratio allows one to vary the parameter A in a broad range, the effect of relativistic self-focusing on the propagation of the laser pulse remaining negligible. As A is increased by a factor of nine, which corresponds, for example, to an increase in the gas density $n_H^{(0)}$ from the value 10^{18} cm^{-3} considered above to the value 9×10^{18} cm^{-3} (in this case, $P/P_c \approx 0.13$), the ionisation modulation proves to be considerably more distinct already at the distance $z = 0.1z_R$ (Fig. 9) than the modulation under conditions in Fig. 5. As a result, the space–time distribution of the laser pulse intensity exhibits strong oscillations upon the pulse propagation inside the matter (Fig. 10), and the shape of the distribution at $z = 0.3z_R$ becomes close to that obtained in paper [14] (see Fig. 10c). Note that the parameters used in Figs 9 and 10 correspond to $\delta \approx 12 \gg 1$ [see (17)]. Under these conditions, one cannot expect the formation of a step profile and its subsequent propagation deep into the ionising

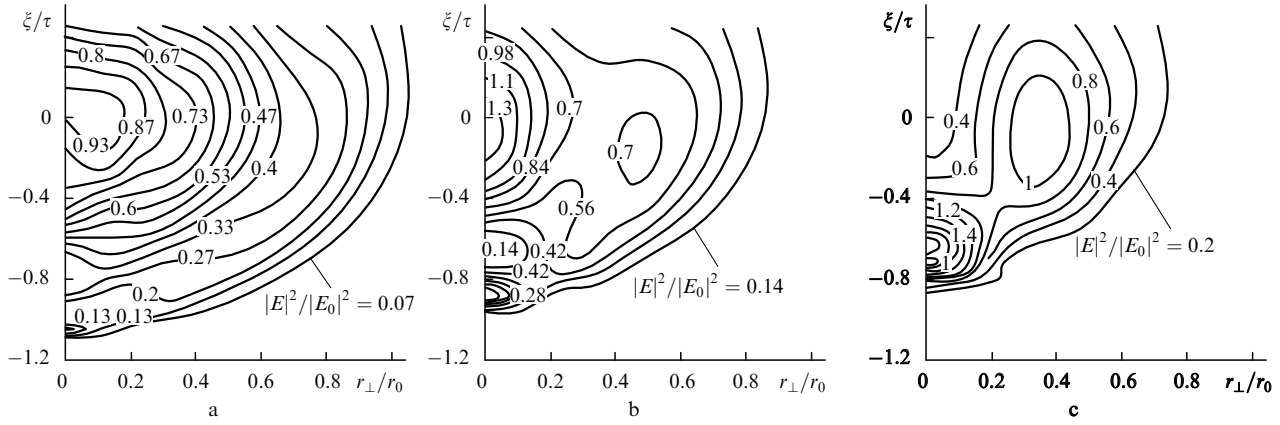

Figure 10. Level lines $|E(s, r_\perp, \xi)|^2/|E_0|^2$ in the pulse frame of reference $\xi, r_\perp$ for $z = 0.1z_R$ (a), $0.2z_R$ (b), and $0.3z_R$. The parameters of the pulse and gas are as in Fig. 9.

matter, in complete accordance with the predictions of the model proposed above.

5. Conclusions

Upon propagation of a laser pulse into an ionising matter, the temporal profile of the pulse becomes modulated. The modulation is excited upon ionisation of neutral particles or ions with different ionisation degrees and is caused by the refraction of an electromagnetic radiation from inhomogeneous plasma bunches produced during the ionisation of the matter by the spatially inhomogeneous pulse. In gases with many-electron atoms, the successive ionisation occurs at different intensities of laser radiation and, hence, the modulation is initiated in different regions of the temporal profile of the pulse.

The modulation amplitudes in different regions of the temporal profile of the laser pulse first increase and then decrease upon the pulse penetration deep into the matter. The maxima of the relative modulation amplitudes are achieved at the penetration depth $z_{st} = z_R/u^{(2)} \approx 0.3z_R$. The maximum relative modulation amplitude is determined by expression (17) and increases with the radius of the laser beam and the free-electron density. The position of the modulation maximum on the laser-pulse profile is determined by expression (15) for $n = 2$ and $s = 1/u^{(2)}$. If this position coincides with the initial position of the peak intensity I_0 [i.e., $\xi_{ak}^{(2)} = 0$ in (15)], then the maximum intensity of the pulse increases. The relative increase in the maximum intensity compared to the initial intensity I_0 can be estimated from expression (17) and can be significant. Such a 'resonance' at the penetration depth z_{st} is possible when $\xi_{ak}^{(2)} = 0$ and, hence, $I_{ak}^{th} = I_0 \exp(-2)$ [see (15)]. This relation can be satisfied for a particular gas by a proper choice of the peak intensity I_0.

Acknowledgements. This work was partially supported by the Russian Foundation for Basic Research (Grant No. 01-02-16723).

References

1. Andreev N.E., Chegotov M.V., Veisman M.E. *IEEE Trans. Plasma Sci.*, **28**, 1098 (2000).
2. Andreev N.E., Veisman M.E., Keidzhyan M.G., Chegotov M.V. *Fiz. Plazmy*, **26**, 1010 (2000).
3. L'Huillier A., Lompre L.-A., Mainfray G., Manus C., in *Atoms in intense laser fields*. Ed. by M.Gavrila (New York, Academic Press, 1992) p. 139 – 201.
4. Andreev N.E., Chegotov M.V. *Proc. SPIE Int. Soc. Opt. Eng.*, **4352**, 191 (2001).
5. Sprangle P., Esarey E., Hafizi B. *Phys. Rev. Lett.,* **79**, 1046 (1997).
6. Sprangle P., Esarey E., Hafizi B. *Phys. Rev. E*, **56**, 5894 (1997).
7. Bespalov V.I., Talanov V.I. *Pis'ma Zh. Eksp. Teor. Fiz.*, **3**, 471 (1966).
8. Antonsen T.M., Bian Z. *Phys. Rev. Lett.*, **82**, 3617 (1999).
9. Chegotov M.V. *Fiz. Plazmy*, **26**, 940 (2000).
10. Malka V., De Wispelaere E., Marques J.R., et al. *Phys. Plasmas*, **3**, 1682 (1996).
11. Leemans W.P., Clayton C.E., Mori W.B., et al. *Phys. Rev. A*, **46**, 1091 (1992).
12. Couairon A., Berge L. *Phys. Plasmas*, **7**, 193 (2000).
13. Couairon A., Berge L. *Phys. Plasmas*, **7**, 210 (2000).
14. Chessa P., De Wispelaere E., Dorchies F., et al. *Phys. Rev. Lett.*, **82**, 552 (1999).
15. Ammosov M.V., Delone N.B., Krainov V.P. *Zh. Eksp. Teor. Fiz.*, **91**, 2008 (1986).
16. Abramowitz M., Stegun I.A. (Eds) *Handbook of Mathematical Functions* (New York: Dover, 1965; Moscow: Nauka, 1979).